Cup Products on Polyhedral Approximations of 3D Digital Images

Rocio Gonzalez-Diaz[1], Javier Lamar[2], and Ronald Umble[3]

[1] Dept. of Applied Math (I), School of Computer Engineering, University of Seville, Campus Reina Mercedes, C.P. 41012, Seville, Spain
rogodi@us.es

[2] Pattern Recognition Department, Advanced Technologies Application Center, 7th Avenue #21812 218 and 222, Siboney, Playa, C.P. 12200, Havana City, Cuba
jlamar@cenatav.co.cu

[3] Department of Mathematics, Millersville University of Pennsylvania, P.O. Box 1002 Millersville, PA 17551-0302, Pennsylvania, USA
ron.umble@millersville.edu

Abstract. Let I be a 3D digital image, and let $Q(I)$ be the associated cubical complex. In this paper we show how to simplify the combinatorial structure of $Q(I)$ and obtain a homeomorphic cellular complex $P(I)$ with fewer cells. We introduce formulas for a diagonal approximation on a general polygon and use it to compute cup products on the cohomology $H^*(P(I))$. The cup product encodes important geometrical information not captured by the cohomology groups. Consequently, the ring structure of $H^*(P(I))$ is a finer topological invariant. The algorithm proposed here can be applied to compute cup products on any polyhedral approximation of an object embedded in 3-space.

Keywords: Cellular complex, cohomology, cup product, diagonal approximation, digital image, polyhedron.

1 Introduction

Throughout this paper, coefficients lie in the field $\mathbb{Z}_2$. Let X be a cellular complex embedded in 3-dimensional space and constructed by gluing 3-dimensional polyhedra together along common faces (see [4]). At a most basic level, the connected components, homotopy classes of non-contractible loops, and boundaries of tunnels in X generate the cellular cohomology $H^*(X)$. At the next level, certain relationships among the generators are encoded by the cup product, which endows $H^*(X)$ with a graded commutative ring structure. Indeed, the discriminating information encoded by the cup product improves our capability to distinguish between 3D images. For example, $H^*(S^1 \vee S^1 \vee S^2)$ and $H^*(S^1 \times S^1)$ are isomorphic as vector spaces but not as rings since cup products vanish in the wedge but not in the product. Thus $S^1 \vee S^1 \vee S^2$ and $S^1 \times S^1$ have quite different topological properties.

To date, the cup product has seen limited application to problems in 3D image processing. In [10,11], Gonzalez-Diaz and Real used their 14-adjacency algorithm

J.K. Aggarwal et al. (Eds.): IWCIA 2011, LNCS 6636, pp. 107–119, 2011.

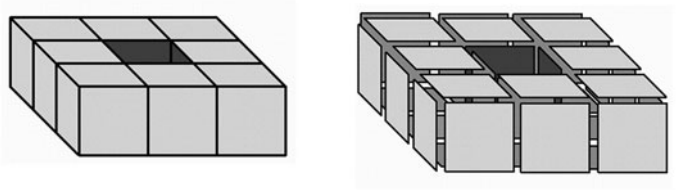

Fig. 1. Left: A digital image $I = (\mathbb{Z}^3, 26, 6, B)$; the set B consists of 8 unit cubes (voxels). Right: The quadrangles of $\partial Q(I)$.

and the standard formulation in [17] to compute cup products on the simplicial complex $K(I)$ associated with a given digital image I. More recently, Gonzalez-Diaz, Jimenez and Medrano introduced a method for computing cup products on cubical approximations $Q(I)$. Their cup products are computed directly from the cubical complex, and no additional subdivisions are necessary [8,9]. For a geometrical interpretation of cohomology in the context of digital images, we refer the reader to [5,6,15].

In [14], Kravatz computed cup products on a general 2-dimensional polygon in terms of a combinatorial *diagonal approximation*, which assumes a particular ordering of the vertices. In this paper, we introduce a more general formula for computing cup products, which is independent of the ordering of vertices and computationally effective.

A problem that frequently arises in 3D image processing is to efficiently encode the boundary surface of a given digital object as a set of voxels. The most popular approach to this problem uses a triangulation. While triangles are combinatorially simple, and visualization of triangulated surfaces is supported by existing hardware and software, the number of triangles required is often large and the computational analysis correspondingly slow. It is desirable, therefore, to seek more computationally economical combinatorial approximations. Adjacent coplanar triangles in a triangulation, for example, can be merged into more general polygons and become faces of more general but combinatorially simpler polyhedra. The payoff from combinatorial simplicity is improved computational efficiency.

Approximating 3D objects with polyhedral complexes is a well-studied problem in the field of Computational Geometry (for example, see [1,2,3]). An algorithm for constructing polyhedral approximations in certain special cases was given by Kovalevsky and Schulz in [13,19]. Their algorithm generates the convex hull of a given object then modifies the convex hull by recursively generating convex hulls of either subsets of the given voxel set or subsets of the background voxels. The result of this method is a polyhedron that separates object voxels from background voxels.

The computational methods introduced in this paper can be effectively applied to any polyhedral approximation of a 3D object. Indeed, one maximizes computational efficiency by approximating a given 3D object with a polyhedral

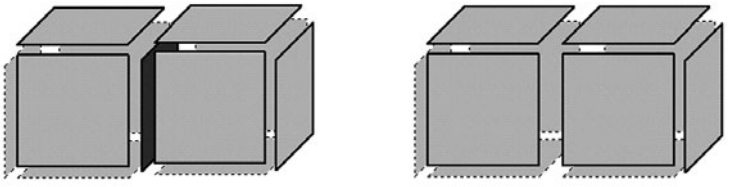

Fig. 2. Left: Quadrangles in the boundary of cubes c and σ sharing a square σ' (in bold). Right: Quadrangles in $\partial(c) := \partial(c + \sigma)$, the boundary of the cell c after removing σ'.

complex containing a minimal number of cells. To the extent that this is our long-term objective, we take a first step in this direction here.

The paper is organized as follows: In Section 2 we introduce a simplification procedure, which produces a cellular complex $P(I)$ homeomorphic to $Q(I)$ with significantly fewer cells. In Section 3 we define a diagonal approximation on a general polygon and use it to compute the cohomology ring of $P(I)$. Conclusions and some ideas for future work are discussed in Section 4.

2 3D Digital Pictures and Cellular Complexes

Let I be a 3D digital image and let $Q(I)$ be an associated cubical complex. In this section we introduce a simplification procedure, which produces a cellular complex $P(I)$ homeomorphic to $Q(I)$ with significantly fewer cells.

Intuitively, a *cellular decomposition* of a 3D space X embedded in $\mathbb{R}^3$ is a representation of X as a finite union of vertices (0-*cells*), edges (1-*cells*), polygons (2-*cells*), and polyhedra (3-*cells*), which have been glued together in such a way that the non-empty intersection of two cells is a cell. A k-cell is also referred to as a k-*face*. A *cellular complex* is a 3D space X embedded in $\mathbb{R}^3$ together with a cellular decomposition. For a precise definition of a cellular complex, which is more subtle than one might expect, see [4].

A *cubical complex* Q is a cellular complex whose 2-cells are squares (or quadrangles) and whose 3-cells are cubes. Note that if a cube is in Q, its bounding quadrangles are in Q; if a quadrangle is in Q, its bounding edges are in Q; and if an edge is in Q, its endpoints are in Q.

Consider a 3D binary digital picture $I = (\mathbb{Z}^3, 26, 6, B)$, where $\mathbb{Z}^3$ is the underlying grid and B (the foreground) is a finite set of points of the grid fixing the 26-adjacency for the points of B and the 6-adjacency for the points of $\mathbb{Z}^3 \setminus B$ (the background). The cells of $Q(I)$ are unit cubes centered at the points of B with faces parallel to the coordinate planes (called the *voxels* of I), together with their quadrangles, edges, and vertices.

Let K be a cellular complex. An i-cell $\sigma' \in K$ is a *facet* of a cell $\sigma \in K$ if σ is an $(i+1)$-cell and σ' is a face of σ. A *maximal* cell of K is not a facet of any cell of K. The boundary of K, denoted by ∂K, is the subcomplex of K consisting of all cells that are facets of exactly one (maximal) cell, and their faces. Note that

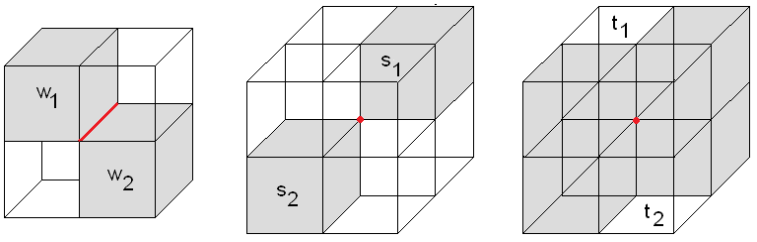

Fig. 3. Critical configurations (i), (ii) and (iii) (modulo reflections and rotations)

the maximal cells of $\partial Q(I)$ are all the quadrangles of $Q(I)$ shared by a voxel of B and a voxel of $\mathbb{Z}^3 \setminus B$ (see Figure 1).

Following the exposition in [8,9], given a digital image I and its associated cubical complex $Q(I)$, we apply a face-reduction technique to reduce the number of cells in $Q(I) \setminus \partial Q(I)$ and obtain a cellular complex $K(I)$ homeomorphic to $Q(I)$ whose maximal cells are the quadrangles of $\partial Q(I)$ (see Figure 2 and Algorithm 1). Then, $\partial K(I) = \partial Q(I)$.

```
INPUT: A cubical complex Q(I) associated to a 3D digital image I.
Initially, K(I) := Q(I).
While there exists a cell σ' ∈ Q(I) \ ∂Q(I) do
      If σ' is a facet of exactly two cells c, σ ∈ Q(I) do
         remove σ and σ' from the current K(I);
         redefine c as c ∪ σ.
      If σ' is a facet of exactly one cell σ ∈ Q(I) do
         remove σ and σ' from the current K(I).
OUTPUT: the cellular complex K(I).
```

Algorithm 1. Face-Reduction Process

Next, we preform a simplification process in $\partial K(I)$ to produce a cellular complex $P(I)$ homeomorphic to $K(I)$ such that the maximal cells of $\partial P(I)$ are polygons. But first, we need a definition.

Definition 1. *A vertex $v \in \partial K(I)$ is **critical** if one of the following situations occurs:*

(i) v is a face of some edge e shared by four cubes, exactly two of which intersect along e and lie in $Q(I)$ (see cubes w_1 and w_2 in Figure 3).
(ii) v is shared by eight cubes, exactly two of which are are corner-adjacent and contained in $Q(I)$ (see cubes s_1 and s_2 in Figure 3).
(iii) v is shared by eight cubes, exactly two of which are corner-adjacent and not contained in $Q(I)$ (cubes t_1 and t_2 in Figure 3).

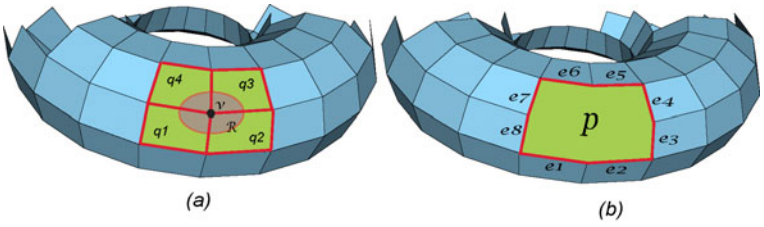

Fig. 4. (a) $N_v \leftarrow \{q1, q2, q3, q4\}$, (b) facets of $p \leftarrow \{e1, e2, e3, e4, e5, e6, e7, e8\}$

It is a well-known fact that a non-critical vertex of $\partial K(I)$ lies in a neighborhood of $\partial K(I)$ homeomorphic to $\mathbb{R}^2$ (see [16]).

Algorithm 2 processes the non-critical vertices of $\partial K(I)$ to obtain the cellular complex $P(I)$. Initially, $P(I) = K(I)$. For a vertex $v \in \partial P(I)$, let N_v be the set of 2-cells $q \in P(I)$ incident to the vertex v. If N_v defines a region R_v homeomorphic to a disc, then N_v is replaced by a new 2-cell p in $P(I)$, which is the union of the cells of N_v. The edges of $\partial P(I)$ incident to v and the vertex v are removed from $P(I)$ (see Figure 4). Observe that the maximal cells of the final cellular complex $\partial P(I)$ are polygons and $\partial P(I)$ has fewer cells than $\partial K(I)$. We can set some terminating conditions. For example: (1) terminate when the number of edges of the polygons in $\partial P(I)$ reach some specified maximum; or (2) terminate after merging the set N_v of coplanar 2-cells of $\partial P(I)$ (this preserves the geometry but removes fewer cells). An example of the differences that arise from these different terminating conditions is demonstrated in Example 1.

Observe that Algorithm 2 uses the ordering on the set of non-critical vertices $V \subset \partial K(I)$ to select the next non-critical vertex. To the best of our knowledge, this is the first algorithm to appear that produces a cellular complex with polygonal maximal cells by removing non-critical vertices.

Example 1. Let μI be a μMRI of a trabecular bone of size: $85 \times 85 \times 10$ voxels (see Figure 5 in which μI is given by a sequence of 10 2D digital images of size

```
INPUT: The output of Algorithm 1: the cellular complex K(I).
Initially, P(I) := K(I);
          V := ordered set of non-critical vertices of ∂K(I).
While ∃v ∈ V such that R_v is homeomorphic to a disc do
      remove v from P(I) and V;
      remove the edges incident to v from P(I);
      remove the 2-cells of N_v from P(I);
      add a new 2-cell p to P(I) which is the union of the cells of N_v.
OUTPUT: The cellular complex P(I).
```

Algorithm 2. Algorithm to obtain the cellular complex $P(I)$

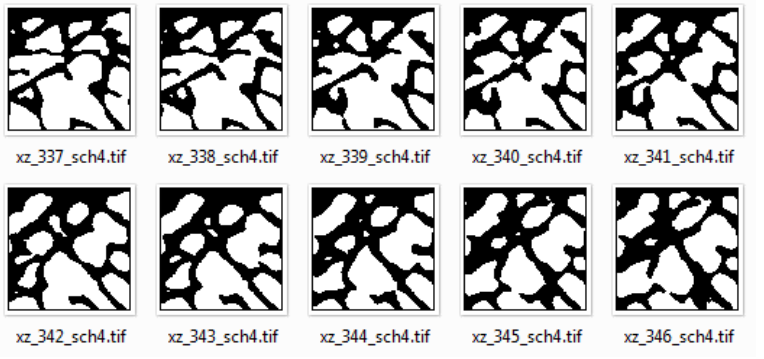

Fig. 5. A μMRI of a trabecular bone

85×85). The number of quadrangles in $\partial Q(\mu I)$ is 20956 (see Figure 6). After applying Algorithm 1 to obtain the cellular complex $K(\mu I)$, we apply Algorithm 2 to $K(\mu I)$ with the terminating condition 1 (the number of the edges of the polygons in $\partial P(\mu I)$ is smaller or equal to 10). Then, the number of polygons of $\partial P(\mu I)$ is 1567 (see Figure 7.a). If we only consider the set of coplanar polygons N_v, then the number of polygons of $\partial P(\mu I)$ after applying Algorithm 2 is 9321 (see Figure 7.b).

3 Computing the Cohomology Ring of $P(I)$

Traditionally, one computes cup products in simplicial or cubical complex using the standard formulas in [17,20]). In this section, we give a procedure for computing cup products on $P(I)$ (the output of Algorithm 2), which avoids triangulation by defining explicit formulas for diagonal approximations on polygons.

We begin with a review of some standard definitions from Algebraic Topology (for details see [17]). Given a graded set $S = \{S_q\}_q$, the *q-chains* of S, which are finite formal sums of elements of S_q, define an additive abelian group structure on S_q. These groups, called *q-chain groups*, are denoted by $C_q(S)$. The collection of all chain groups associated with S is denoted by $C_*(S) = \{C_q(S)\}_q$

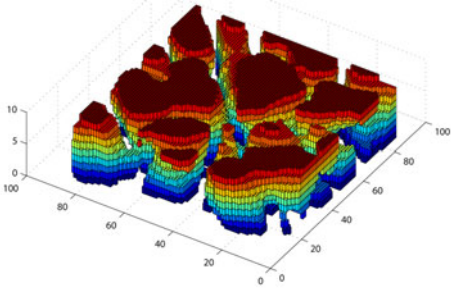

Fig. 6. The cubical complex $\partial Q(\mu I)$

and is referred to as the *chain group of* S. A *chain complex* $(C_*(S), \partial)$ is a chain group $C_*(S)$ together with a square zero homomorphism $\partial = \{\partial_q : C_q(S) \to C_{q-1}(S)\}_q$, called the *boundary operator*. For example, consider a triangle $\langle v_i, v_j, v_k\rangle$ with vertices $v_i < v_j < v_k$. The boundary of the triangle is the formal sum of its edges, that is, $\partial_2(\langle v_i, v_j, v_k\rangle) = \langle v_i, v_j\rangle + \langle v_j, v_k\rangle + \langle v_i, v_k\rangle$. Note that any chain group $C_*(S)$ together with the zero boundary map $\partial \equiv 0$ is a chain complex.

The chain complex associated with $P(I)$ (the output of Algorithm 2) is the collection $(C_*(P(I)), \partial) = \{C_q(P(I)), \partial_q\}_q$ where:

- each $C_q(P(I))$ is the chain group generated by the q-cells of $P(I)$,
- the boundary $\partial_q : C_q(P(I)) \to C_{q-1}(P(I))$ evaluated on a q-cell of $P(I)$ is the formal sum of its facets, and
- the boundary of a general q-chain is defined by linearly extending ∂.

Given a chain complex $(C_*(S), \partial)$, a q-chain $\sigma \in C_q(S)$ is called a *q-cycle* if $\partial_q(\sigma) = 0$. If $\sigma = \partial_{q+1}(\mu)$ for some $(q+1)$-chain μ then σ is called a *q-boundary*. Referring to the triangle $\langle v_i, v_j, v_k\rangle$ above, $\sigma = \langle v_i, v_j\rangle + \langle v_j, v_k\rangle + \langle v_i, v_k\rangle$ is both a 1-cycle and a 1-boundary since $\partial_1(\sigma) = 0$ and $\sigma = \partial_2(\langle v_i, v_j, v_k\rangle)$.

Two q-cycles a and a' are *homologous* if there exists a q-boundary b such that $a = a' + b$. Denote the groups of q-cycles and q-boundaries by $Z_q(S)$ and $B_q(S)$, respectively. All q-boundaries are q-cycles ($B_q(S) \subseteq Z_q(S)$). Define the *q^{th} homology group* to be the quotient group $H_q(S) = Z_q(S)/B_q(S)$, for all q. Each element of $H_q(S)$ is a class $[a] = a + B_q(S)$ and a is a *representative q-cycle*. The *homology* of S is the collection of all the homology groups associated with S, i.e., $H_*(S) = \{H_q(S)\}_q$.

Let $(C_*(S), \partial)$ and $(C_*(S'), \partial')$ be chain complexes. A homomorphism $f = \{f_q : C_q(S) \to C_q(S')\}_q$ such that $f_q\partial_q = \partial'_q f_q$ for all q is a *chain map*. Note that the identity $id_{C_*(S)} = \{id_{C_q(S)} : C_q(S) \to C_q(S)\}_q$ is a chain map.

Let $f = \{f_q : C_q(S) \to C_q(S')\}_q$ and $g = \{g_q : C_q(S) \to C_q(S')\}_q$ be chain maps. A *chain homotopy from f to g* is a homomorphism $\phi = \{\phi_q : C_q(S) \to C_{q+1}(S')\}_q$ such that $\phi_{q-1}\partial_q + \partial'_{q+1}\phi_q = f_q + g_q$ for all q. A *chain contraction of $(C_*(S), \partial)$ to $(C_*(S'), \partial')$* is a triple ($f = \{f_q : C_q(S) \to C_q(S')\}_q$, $g = \{g_q : C_q(S') \to C_q(S)\}_q$, $\phi = \{\phi_q : C_q(S) \to Cq + 1(S)\}_q$) such that

(i) f and g are chain maps;
(ii) ϕ is a chain homotopy from $id_{C_*(S)}$ to $gf = \{g_q f_q : C_q(S) \to C_q(S)\}_q$;
(iii) $fg = \{f_q g_q : C_q(S') \to C_q(S')\}_q = id_{C_*(S')}$.

Cochain groups are the linear duals of chain groups. Given a chain complex $(C_*(S), \partial)$, a *q-cochain* $c \in Hom(C_q(S), \mathbb{Z}/2)$. If we index the q-cells in a cellular complex from 1 to n_q, their corresponding duals generate $C_*(S)$. Thus a cochain $c \in C_*(S)$ is a $\mathbb{Z}_2$-linear combination of the n_q elements in the dual basis, and as such can be thought of as a bit string of length n_q.

The set $C^q(S)$ of all q-cochains is a group, and the direct sum of all cochain groups associated with S is the graded group $C^*(S) = \{C^q(S)\}_q$. The *coboundary operator* $\delta = \{\delta^q : C^q(S) \to C^{q+1}(S)\}_q$ is defined on a q-cochain c by $\delta^q(c) = c\partial_{q+1}$. Note that $\delta \circ \delta = 0$. The associated *cochain complex* is the pair $(C^*(S), \delta)$.

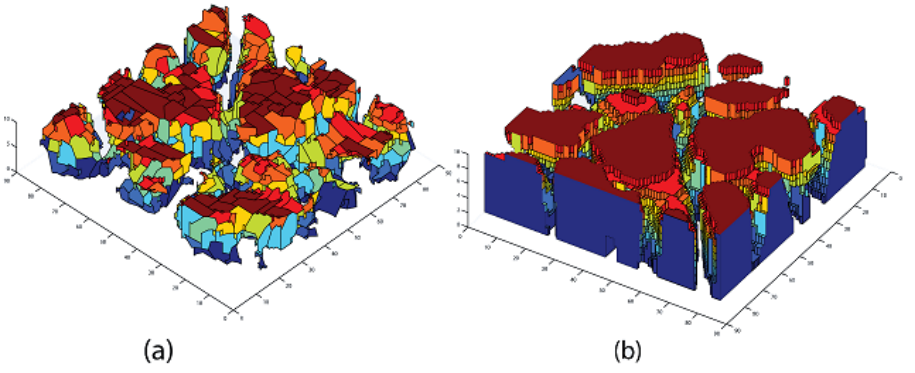

Fig. 7. (a) The cellular complex $\partial P(\mu I)$ for 10 edges as upper bound on $p \in \partial P(\mu I)$. (b) The cellular complex $\partial P(\mu I)$ preserving geometry.

A q-cochain c is a q-cocycle if $\delta^q(c) = 0$. A q-cochain b is a q-coboundary if there exists a $(q-1)$-cochain c such that $b = \delta^{q-1}(c)$. Two q-cocycles c and c' are *cohomologous* if there exists a q-coboundary b such that $c = c' + b$ (see Figure 8). We denote the subgroup of q-cocycles by $Z^q(S)$, and the subgroup of q-coboundaries by $B^q(S)$. The q^{th} *cohomology group* is defined to be the quotient $H^q(S) = Z^q(S)/B^q(S)$. Each element of $H^q(S)$ is a class $[c] = c + B^q(S)$. The element c is a *representative q-cocycle* of the cohomology class $[c]$. The *cohomology* of S is the graded $\mathbb{Z}/2$-vector space $H^*(S) = \{H^q(S)\}_q$.

Since $P(I)$ (the output of Algorithm 2) is embedded in $\mathbb{R}^3$, homology and cohomology of $P(I)$ are isomorphic and torsion free.

An *AT-model* [10,11] for a chain complex $(C_*(S), \partial)$, denoted by $((S, \partial), H, f, g, \phi)$, consists of a chain complex $(C_*(H), \partial' \equiv 0)$ together with a chain contraction (f, g, ϕ) of $(C_*(S), \partial)$ to $(C_*(H), \partial')$. The following properties hold:

- If $\sigma \in H_q$, then $g_q(\sigma) \in C_q(S)$ is a representative cycle of a class of $H_q(C(S))$.
- The cochain $\partial_\sigma f : C_q(S) \to \mathbb{Z}/2$ defined by

$$\partial_\sigma f(\mu) := \begin{cases} 1, & \text{if } \sigma \text{ appears in the expression of } f(\mu), \\ 0, & \text{otherwise;} \end{cases}$$

  is a representative cocycle of a class of $H^q(S)$.

- The map $H_q \to H_q(S)$ given by $\sigma \mapsto [g(\sigma)]$ linearly extends to an isomorphism $C_q(H) \cong H_q(S)$.
- The map $H_q \to H^q(S)$ given by $\sigma \mapsto [\partial_\sigma f]$ linearly extends to an isomorphism $C_q(H) \cong H^q(S)$.

Example 2. Consider the cellular complex $\partial P(\mu I)$ shown in Figure 7.b obtained after applying Algorithm 2 to a μMRI of a trabecular bone of size $85 \times 85 \times 10$

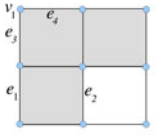

0-cochain	$\{v_1\}$
1-cochain	$\{e_1, e_4\}$
1-coboundary	$\delta\{v_1\} = \{e_3, e_4\}$
1-cocycle	$c = \{e_1, e_2\}$
1-cocycle	$d = \{e_1, e_2, e_3, e_4\}$
homologous cocycles	c and d; since $d = c + \delta\{v_1\}$

Fig. 8. Example of cochain, cocycle and coboundary

voxels. Table 1 shows the results of the homology computation, i.e, the number of connected components, holes and cavities obtained after computing an AT-model for $\partial P(\mu I)$. Representative 1-cycles are shown in Figure 9.

Table 1. Results of the homology groups computation for the cellular complex $\partial P(\mu I)$ shown in Figure 7.b. (see Figure 9).

Cellular Complex	H_0	H_1	H_2
$\partial P(\mu I)$	5	2	6

An AT-model for $(C_*(S), \partial)$ always exists and can be computed in $\mathcal{O}(m^3)$, where m is the number of elements of S (see [10,11]).

Given an AT-model $((P(I), \partial), H, f, g, \phi)$ for $P(I)$ (the output of Algorithm 2), we have that

$$C_*(H) \cong H_*(P(I)) \cong H^*(P(I)) \cong Hom\,(H_*(P(I)), \mathbb{Z}/2) \cong C^*(H).$$

Let $\alpha \in H_n$. Consider the dual *elementary n-cocycle* in $C^n\,(H)$,

$$\alpha^* : C_n(H) \to \mathbb{Z}/2 \quad \text{such that for } \mu \in H_n, \quad \alpha^*(\mu) := \begin{cases} 1 & \text{if } \mu = \alpha, \\ 0 & \text{otherwise.} \end{cases}$$

Proposition 1. *Given an ordering* $\{v_1 < \cdots < v_n\}$ *of the vertices of* $P(I)$*, each polygon* $p \in P(I)$ *can be expressed as an ordered list of vertices* $\{v_{i_1} < \cdots < v_{i_k}\} \subseteq \{v_1 < \cdots < v_n\}$ *with edges*

$$e_j := \begin{cases} \langle v_{i_j}, v_{i_{j+1}} \rangle, & \text{if } j < k, \\ \langle v_{i_k}, v_{i_1} \rangle, & \text{if } j = k. \end{cases}$$

The following two theorems formulate a diagonal approximation ∇' on a polygon and the cup product on $H^*(P(I))$ in terms of ∇'. All non-trivial cup products in $H^*(P(I))$ are products of 1-cocycles for dimensional reasons.

Theorem 1. *Consider a polygon* $p = \langle v_1, \ldots, v_n \rangle$ *with edges* $e_i = \langle v_i, v_{i+1} \rangle$*,* $i < n$*, and* $e_n = \langle v_n, v_1 \rangle$*. Then a diagonal approximation on* p *is given by*

$$\begin{aligned} \nabla'(p) := & \textstyle\sum_{1<i<n,\, v_i<v_{i+1}} (e_1 + \cdots + e_{i-1}) \otimes e_i \\ & + \textstyle\sum_{1<i<n,\, v_i>v_{i+1}} (e_{i+1}) + \cdots + e_n) \otimes e_i. \end{aligned}$$

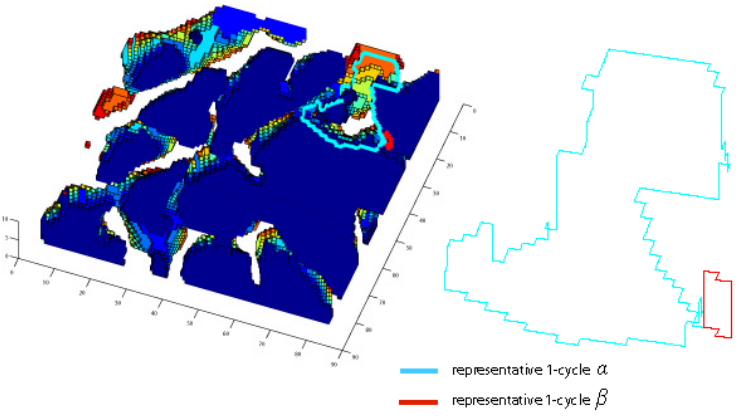

Fig. 9. Representative 1-cycles

Theorem 2. *Consider a digital image I, the cellular complex $P(I)$, an ordering of the vertices of $P(I)$, and an AT-model $((P(I), \partial), H, f, g, \phi)$ for $P(I)$. Then for $\alpha, \beta \in H_1$ and $\gamma \in H_2$ the* cup product $\alpha^* \smile' \beta^*$ *is given by*

$$(\alpha^* \smile' \beta^*)(\gamma) = m(\partial_\alpha f \otimes \partial_\beta f)\nabla' g(\gamma), \tag{1}$$

where m denotes multiplication in $\mathbb{Z}/2$. The cup product is bilinear, commutative, associative, and independent of the ordering of the vertices .

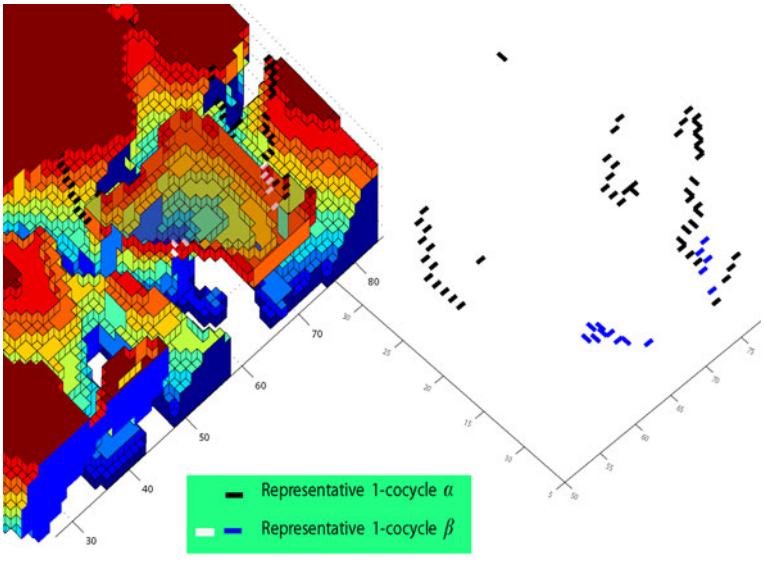

Fig. 10. Representative 1-cocycles

Table 2. Results of the computation of the cup product for the cellular complex shown in Figure 7.b

	$(\alpha\ ,\ \alpha)$	$(\alpha\ ,\ \beta)$	$(\beta\ ,\ \beta)$
γ_1	0	0	0
γ_2	0	0	0
γ_3	0	0	0
γ_4	0	0	0
γ_5	0	0	0
γ_6	0	1	0

Table 3. Time (in seconds) and the results of the computation of the cup product on the cellular complexes shown in Figure 11

Cell complex	Number of 2-cells	Time to compute the cup product
A (see Figure 11)	1920	18.19 sec.
B (see Figure 11)	57	3.8 sec.

	$(\alpha_1\ ,\ \alpha_2)$	$(\alpha_1\ ,\ \alpha_3)$	$(\alpha_1\ ,\ \alpha_4)$	$(\alpha_2\ ,\ \alpha_3)$	$(\alpha_2\ ,\ \alpha_4)$	$(\alpha_3\ ,\ \alpha_4)$
β	0	0	1	1	0	0

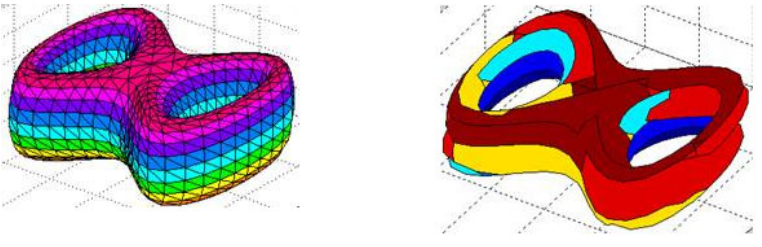

Fig. 11. Left: cell complex A. Right: cell complex B

Proof. (Sketch) To verify formula (1), we subdivide the polygons of $P(I)$, obtain a very special triangulation K of $P(I)$, and apply a chain contraction (f_T, g_T, ϕ_T) of $C_*(K)$ to $C_*(P(I))$ (we only need to subdivide the polygons of $P(I)$ since the cup product is non-trivial only on 1-cocycles). We then appeal to the standard formula on a triangle with vertices $v_i < v_j < v_k$ (see [17]):

$$\nabla(\langle v_i, v_j, v_k\rangle) = \langle v_i, v_j\rangle \otimes \langle v_j, v_k\rangle.$$

Finally, for a polygon $p \in P(I)$ we have $\nabla'(p) = (f_T \otimes f_T)\nabla g_T(p)$. □

Example 3. Starting from the results obtained in Example 2 and applying the formula given in Theorem 2, representative 1-cocycles are shown in Figure 10. Table 2 shows the cup product.

The following table illustrates the dramatic improvement in computational efficiency realized by removing faces and non-critical vertices:

4 Conclusions and Plans for Future Work

Given a 3D digital image I, we have formulated the cup product on the cohomology of the cellular complex $P(I)$ obtained by simplifying the cubical complex $Q(I)$. The algorithm proposed here is valid for any encoding of a 3D digital object given as a set of polyhedra. Nevertheless, our ultimate goal is to compute the cup product on any cellular complex without making use of triangulations or other kind of subdivision. To this end, we shall apply some standard geometric constructions such as forming quotients, taking Cartesian products, and merging cells.

References

1. Argawal, P.K., Suri, S.: Surface approximation and geometric partitions. SIAM Journal on Computing 27(4), 1016–1035 (1998)
2. Brönnimann, H., Goodrich, M.T.: Almost optimal set covers in finite VC-dimension. Discrete and Computational Geometry 14, 263–279 (1995)
3. Das, G., Goodrich, M.T.: On the complexity of optimization problem for 3D convex polyhedra and decision trees. Computational Geometry: Theory and Applications 8, 123–137 (1997)
4. Hatcher, A.: Algebraic Topology. Cambridge University Press, Cambridge (2002)
5. Gonzalez-Diaz, R., Ion, A., Iglesias-Ham, M., Kropatsch, W.: Irregular graph pyramids and representative cocycles of cohomology generators. In: Torsello, A., Escolano, F., Brun, L. (eds.) GbRPR 2009. LNCS, vol. 5534, pp. 263–272. Springer, Heidelberg (2009)
6. Gonzalez-Diaz, R., Ion A., Iglesias-Ham M., Kropatsch W.: Invariant representative cocycles of cohomology generators using irregular graph pyramids. Computer Vision and Image Understanding (in press)
7. Gonzalez-Diaz, R., Jimenez, M.J., Medrano, B., Molina-Abril, H., Real, P.: Integral operators for computing homology generators at any dimension. In: Ruiz-Shulcloper, J., Kropatsch, W.G. (eds.) CIARP 2008. LNCS, vol. 5197, pp. 356–363. Springer, Heidelberg (2008)
8. Gonzalez-Diaz, R., Jimenez, M.J., Medrano, B.: Cohomology ring of 3D cubical complexes. In: IWCIA 2009. LNCS, vol. 5852, pp. 139–150. Springer, Heidelberg (2009)
9. Gonzalez-Diaz, R., Jimenez, M.J., Medrano, B.: Cohomology ring of 3D photographs. Int. Journal of of Imaging Systems and Technology (in press)
10. Gonzalez–Diaz, R., Real, P.: Towards digital cohomology. In: Nyström, I., Sanniti di Baja, G., Svensson, S. (eds.) DGCI 2003. LNCS, vol. 2886, pp. 92–101. Springer, Heidelberg (2003)

11. Gonzalez-Diaz, R., Real, P.: On the cohomology of $3D$ digital images. Discrete Applied Math. 147, 245–263 (2005)
12. Kaczynski, T., Mischaikow, K., Mrozek, M.: Computational homology. Applied Mathematical Sciences 157 (2004)
13. Kovalevsky, V.A., Schulz, H.: Convex hulls in a 3D space. In: Klette, R., Žunić, J. (eds.) IWCIA 2004. LNCS, vol. 3322, pp. 176–196. Springer, Heidelberg (2004)
14. Kravatz, D.: Diagonal approximations on an n-gon and the cohomology ring of closed compact orientable surfaces. Senior Thesis. Millersville University Department of Mathematics (2008)
15. Lamar-Leon, J., Garcia-Reyes, E., Gonzalez-Diaz, R.: Human gait recognition using topological information. In: Proc. of CTIC (2010); Electronic Journal Image-A, `http://munkres.us.es/` 1(3) (2010). Selected paper invited to submit an extended version to a Special issue devoted to CTIC2010 in Pattern Recognition Letter
16. Latecki, L.J.: 3D well-composed pictures. Graphical Models and Image Processing 59(3), 164–172 (1997)
17. Munkres, J.R.: Elements of Algebraic Topology. Addison-Wesley Co., Reading (1984)
18. Peltier, S., Ion, A., Kropatsch, W.G., Damiand, G., Haxhimusa, Y.: Directly computing the generators of image homology using graph pyramids. Image and Vision Computing 27(7), 846–853 (2009)
19. Schulz, H.: Polyhedral approximation and practical convex hull algorithm for certain classes of voxel sets. Discrete Appl. Math. 157(16), 3485–3493 (2009)
20. Serre, J.P.: Homologie singuliere des éspaces fibrés, applications. Ann. Math. 54, 429–501 (1951)